Transcriptome and translatome analyses reveal the regulatory role of betaine in high fat diet (HFD)-induced hepatic steatosis

Tengda Huang
Guangxi University
Jingsu Yu
Guangxi University
Zupeng Luo
Guangxi University
Lin Yu
Guangxi University
Siqi Liu
Guangxi University
Peng Wang
Guangxi University
Mengting Jia
Guangxi University
Tian Wu
guangxi university
Yurou Zhang
Guangxi University
Weiwei Miao
Guangxi University
Haojie Zhang
Guangxi University
Ziyi Song
Guangxi University
Lei Zhou
Guangxi University
Yixing Li (liyixing39@gxu.edu.cn)
Guangxi University

Research Article

Keywords: Betaine,Transcriptome, RNA-seq, Translatome, RNC-seq, High fat diet, NAFLD

Posted Date: May 18th, 2021

DOI: https://doi.org/10.21203/rs.3.rs-461586/v1

Title: Transcriptome and translatome analyses reveal the regulatory role of betaine in high fat diet (HFD)-induced hepatic steatosis

Authors: Tengda Huang[#], Jingsu Yu[#], Zupeng Luo, Lin Yu, Siqi Liu, Peng Wang, Mengting Jia, Tian Wu, Yurou Zhang, Weiwei Miao, Haojie Zhang, Ziyi Song, Lei Zhou and Yixing Li[*]

Author affiliations: State Key Laboratory for Conservation and Utilization of Subtropical Agro-Bioresources, College of Animal Science and Technology, Guangxi University, Nanning 530004, P.R. China

[#]These authors contributed equally to this work.

[*]Corresponding author: Dr. Yixing Li, State Key Laboratory for Conservation and Utilization of Subtropical Agro-Bioresources, College of Animal Science and Technology, Guangxi University, Nanning 530004, P.R. China. E-mail address: liyixing39@gxu.edu.cn, Tel.: +86 771 323 1158

Abstract:

Non-alcoholic fatty liver disease (NAFLD) is a common disease with a multitude of complications. Increasing evidence shows that the dietary supplement with betaine, a natural chemical molecule, can effectively reduce the fat accumulation in the liver. Translational regulation is considered to play a vital role in gene expression, but whether betaine functions through the regulation of gene translational level is still unclear. To this end, RNC-seq (ribosome-nascent chain complex bound mRNA sequencing) and RNA-seq co-analyses were performed to identify betaine target genes by using the liver samples from high-fat diet + betaine treated and high-fat diet treated mice. The results showed that betaine does play a lipid-lowering role by regulating the expression of gene translation levels; some NAFLD- and lipid metabolism- associated genes were differentially expressed at translational level, for example. And the mRNA translation ratio (TR) of gene significantly increased after betaine treatment. Besides, it is found that the regulation of some genes at transcriptional level is opposite to that at translational level, which indicates that transcriptional regulation and translational regulation may be independent from each other. Finally, we identified several candidate genes, especially *Gpc1*, which may mediate the lipid-lowering effect of betaine in the liver. To sum up, this study depicted the molecular portrait of mice liver with or without betaine treatment from the angel of translatome and transcriptome, giving insights

into the molecular mechanism of betaine-mediated lipid-lowering effect and also providing new clues for understanding and prevention of NAFLD.

Key words: Betaine; Transcriptome; RNA-seq; Translatome; RNC-seq; High fat diet; NAFLD

Introduction

Increasing proof demonstrates that excessive fat/energy intake is related to the risk of developing nonalcoholic fatty liver disease (NAFLD)[1], which is a common form of chronic liver disease[2]. Approximately one-fourth of adults in the world are suffering from NAFLD, which is an increasing threat to human health[3]. This disease is a stress-associated hepatic injury and metabolic disorder featured by diffuse hepatic steatosis and triglyceride accumulation[4,5]. Some vital factors, such as lipid deposition, oxidative stress and inflammatory factors are considered to have significant effects on the occurrence and progression of NAFLD[6], which is linked to obesity[7], insulin resistance (IR)[8], diabetes[9], cardiovascular disease (CVD)[10], nonalcoholic steatohepatitis (NASH)[11], liver cirrhosis[12] and liver cancer[13]. At present, there is no consensus regarding the prevention and treatment of NAFLD, except healthy diet and reasonable exercise, combined with drug adjuvant therapy[14]. Thus, it is urgent to identify potential therapeutic targets, novel drugs and treatment.

Betaine (N,N,N-trimethylglycine, glycine betaine) exists in various common foods，including beets, spinach, chinese wolfberry, wheat, shrimp and shellfish[15-17]. Betaine has been widely used for decades due to its anti-inflammatory, methyl donor, and osmotic pressure regulator effects[18] and has been proven to effectively improve NAFLD[19-24]. As reported,

betaine prevented high fat diet-induced NAFLD by regulating the FGF10/AMPK signaling pathway in ApoE $^{-/-}$ mice[19]. Supplementing betaine after high fat diet-induced NAFLD will make the downstream pathways, which are involved in insulin signal transduction, gluconeogenesis and glycogen synthesis, function normally and improve insulin resistance and steatosis[20]. Betaine, as a methyl donor, alleviates fatty liver induced by corticosterone through epigenetic modification[21]. Betaine attenuates hepatic steatosis by reducing methylation of the MTTP promoter and elevating genomic methylation in mice fed a high fat diet[22]. Betaine has significantly increased mitochondrial content and improved liver lipid metabolism in oleic and palmitic acids induced HepG2 cell[23]. Betaine can improve mitochondrial function in the liver of mouse model with NAFLD caused by methionine and choline, alleviate steatosis, and increase the number of autophagosomes in the mouse's liver[24].

In the process of biological genetic information transmission, translational regulation accounts for more than half of all regulation, which is the most important regulation mode in cells[25,26]. There is insufficient correlation between mRNA abundance and protein abundance, which indicates that there is a certain error in taking gene transcription abundance as protein abundance[27,28]. Therefore, it is not enough to evaluate the change of protein level through the difference of transcription level. Similarly, for proteome, some low-abundance proteins are not well identified by mass

spectrometry (MS), which may lead to some low-abundance proteins with important biological functions not being detected[29]. Consequently, proteomics also has some shortcomings. The purpose of translatome is to study the process of protein production from mRNA translation, which can provide vital information for the translational regulation[30]. Ribosome nascent-chain complex (RNC) bound mRNA (RNC-mRNA) full length sequencing（RNC-seq）is a recently developed method to gaining a genome-wide view of the translational process. The emergence of translatome makes up for the deficiency of transcriptome and proteome, and provides a new perspective for analyzing biological issues. However, at present, the research on translatome is less than that on genomics, transcriptomics and proteomics[31]. Therefore, it is necessary to study translatome.

In this study, the combined analysis of translatome and transcriptome was used to explain betaine alleviate hepatic steatosis induced by high fat diet. Mice were induced into NAFLD model after 17 weeks of high fat diet. Regarding mice, the use of a high fat diet is the preferable model, since the phenotype of NAFLD developed by this model resembles human NAFLD most accurately[32]. Three groups of mice were included. Mice fed with normal fat diet are NFD group; those fed with high fat diet are NAFLD animal models, and this group is called HFD group; those fed with high fat diet and drinking water added with betaine are HB group. Two sequencing

methods, RNA-seq and RNC-seq, were used to explore the differences and associations between transcriptional and translational levels corresponding to this phenotype to further screen out some known target genes and new functional genes. Therefore, this study aims to provide a new direction for the treatment of NFALD through the joint analysis of translatome and transcriptome.

Materials and Methods

Animal and diet

18 Five-week-old C57BL /6 similar weight male mice used in the experiment were purchased from Changsha Tianqin Biotechnology Co., Ltd., Changsha, China, and were acclimated with normal fat diet for 2 weeks. All mice were housed in a controlled environment with a temperature of 24±2℃ and a 12-hour light/dark cycle, with free access to food and water[33]. At week 8, the mice were randomly divided into 3 groups (n=6 in each group), balanced to achieve a similar average body weight. The NFD (control) group was fed with a normal fat diet (11.7% kcal fat). The HFD (NAFLD) group was fed a high fat diet (45% kcal fat; MD12032; Jiangsu Medicience Ltd., Jiangsu, China). The HB (NAFLD + Betaine) group was fed a high fat diet with betaine in drinking water (2% w/v; Beijing Solarbio Science & Technology Co., Ltd., Beijing, China)[19,34]. The mice were sampled in they were 25 weeks old.

MD12032(45% kcal fat): protein 24%, carbohydrates 41%, and fats 24%.

Composition: casein 23.31%, L-cystine 0.35%, corn starch 8.48%, maltodextrin 11.65%, sugar 20.14%, cellulose 5.83%, vegetable oil 2.91%, lard 20.68%, compound minerals3.31%, potassium citrate monohydrate 1.92%, multi-vitamin 1.16%, hydrotartrate choline 0.23%, pigment 0.005%.

Liver sample collection

After feeding the mice to the age of 25 weeks, euthanasia was conducted on them via cervical dislocation after anesthesia. Liver tissues were immediately separated, frozen in liquid nitrogen, and stored at -80℃ for later use.

Triglyceride measurement and Oil Red O staining

Triglyceride (TG) levels in liver samples or cells were measured with an analytical kit (Applygen Technology, Inc., Beijing, China), as directed by the manufacturer. The TG content was normalized to protein concentration that was determined by a BCA protein quantitative analytical kit (P0009; Beyotime Institute of Biotechnology, Shanghai, China).

Liver tissues were prepared into frozen sections, which were stained with Oil Red O (G1016; Wuhan Servicebio Technology Co., Ltd., Wuhan, Hubei, China) for 10 min, and then counter-stained with hematoxylin for 2 min. The slides were viewed at 200× magnification.

RNA extraction

Total RNA was isolated by TRIzol RNA extraction reagent (Ambion, Inc.,

Austin, TX, USA) under the manufacturer's instructions. Total RNA samples were prepared from two independent treatment groups. Equal amount of total RNA from each preparation was pooled respectively, for subsequent library construction and RNA-seq.

RNC-mRNA extraction

Two biological replicates from each group were selected to perform RNC-mRNA extraction. RNC isolation was performed in accordance with a previously reported procedure[31] with some modifications. A total of 90 mg of liver tissues were pre-treated with 100mg/ml cycloheximide for 15 min, followed by pre-chilled phosphate buffered saline washes and addition of 200 μl cell lysis buffer [1% Triton X-100 GBCBIO Technologies Inc., Guangzhou, Guangdong, China] in ribosome buffer （RB buffer） [20 mM HEPES-KOH (pH=7.4), 2 mM dithiothreitol, 15 mM MgCl2, 200 mM KCl and 100 μg/ml cycloheximide] and was homogenized. Another 700 μl lysis buffer was added to the samples, followed by incubation in an ice-bath for 30 min. After centrifuging at 16,200 x g for 20 min at 4°C, supernatants were added to the surface of 5 ml of sucrose buffer (30% sucrose in ribosome buffer), and the RNC complex was pelleted by ultra-centrifugation at 330,000 x g for 3 h at 4°C. RNC-mRNA was extracted from the RNC complex by TRIzol. The quality of the total RNA and RNC-mRNA was detected via electrophoresis with a 2.5% agarose gel.

mRNA sequencing and RNC-mRNA sequencing

The qualified mRNA and RNC-mRNA were subjected to RNA-seq. RNA libraries were prepared according to the protocol of the VAHTS mRNA-seq v.3 Library Prep Kit for Illumina (Vazyme Biotech Co., Ltd, Nanjing, Jiangsu, China), and the raw sequencing reads were generated on an Illumina HiSeqX Ten sequencer.

Sequence analysis

For both mRNA and RNC-mRNA sequencing data sets, high quality reads were mapped to RefSeq mRNA reference sequence (mm10 25-Mar-2017) through the FANSe2 algorithm[35] with the parameters –L80 –E5 –I0 –S14 –B1 –U0. Reads that mapped to alternative splice variants of one gene were merged.

The mRNA and RNC-mRNA in each sample were normalized by RPKM[36] (reads per kilo base per million reads), while relative abundance between two groups was normalized by the edgeR package[37]. Differentially expressed mRNA and RNC-mRNA were identified via the edgeR package with a |fold-change| cutoff of ≥ 2 and FDR cutoff of < 0.01；|fold-change| cutoff of ≥ 2 and FDR cutoff of < 0.05. The TR of a gene of one sample was calculated as previously described: the quotient of the RNC-mRNA RPKM and the mRNA RPKM. Differentially regulated TR was calculated by a t-test with a |fold-change| cutoff of ≥ 2 and p-value cutoff of < 0.05. GO and KEGG were conducted by the Metascape

software for differentially expressed genes.

Cell culture and transient transfection of siRNA

$HepG_2$ cells were maintained in Dulbecco's modified Eagle's medium (DMEM) supplemented with 10% of fetal bovine serum and 1% of antibiotic under an atmosphere of 5% of CO_2 at 37 °C[33]. When there was an 80% confluence, the cells were seeded into 24- or 6-well plates. After 24h, HepG2 cells were divided into three groups: cells in the OA/PA group were cultured with oleic acid (OA, 200 μM) and palmitic acid (PA, 100 μM); cells in the OA/PA + Betaine group were cultured with oleic acid, palmitic acid and betaine (2 mM); cells in the OA/PA +siRNA group were cultured with oleic acid, palmitic acid and transfected with siRNA. The sequences of the siRNAs were as follows, siRNA-*Gpc1*: sense (5'-3'): GAAGCUGGUCUACUGUGCUCACUGC; antisense (3'-5'): GCAGUGAGCACAGUAGACCAGCUUC.

Quantitative Real-Time PCR

Total RNA was extracted from HepG2 cells through a Total RNA Kit I (Omega Bio-tek, Inc., Norcross, GA, USA) and 1 μg of RNA was used as a template for cDNA synthesis via a qRT-PCR system (Bio-Rad, Hercules, CA, U.S.A.). The cDNA was diluted 5-fold with double-distilled water, and SYBR-green-based PCR (GenStar BioSolutions, Beijing, China) was performed with 5 μL cDNA, 2 μL primer (1 μL forward primer and 1 μL reverseprimer), 10 μL SYBR-green mixture (A301 Genstar, Beijing,

China), and 3 μL double-distilled water. Each experiment was repeated at least three times. Gene expression levels were determined with GAPDH as an internal reference. The forward and reverse primers were as follows: *Gpc1*: sense (5'-3'): GCCCTGACTATTGCCGAAATGTG and antisense (3'-5'): GAACTTGTCGGTGATGAGCACC; GAPDH: sense (5'-3'): TGCACCACCAACTGCTTAGC and antisense (3'-5'): GGCATGGACTGTGGTCATGAG.

Statistical analysis

Results of experiments were presented as mean ± the standard deviation (SD). The Student's *t*-test was employed to determine the significance of the difference between two groups, and the one-way analysis of variance （ANOVA）for more than two groups. P-value < 0.05 was considered significant.

Results

Figure 1 shows the experimental design of the present study.

Betaine significantly improved hepatic steatosis in HFD NAFLD mice

After a feeding period of 17 weeks, compared with NFD group, the liver TG level of mice in HFD group increased by twice, which indicates the successful establishment of NAFLD model induced by high fat diet. However, compared with the HFD group, the TG level in the liver of the HB group significantly decreased (Figure 2A). In addition, this result was confirmed by oil red O staining of liver sections (Figure 2B). This indicates

that betaine does alleviate fat deposition induced by high-fat diet.

Overview of RNA-seq and RNC-seq in HFD and HB group mice livers

To investigate the gene expression regulation associated with phenotypes at the translatome and transcriptome levels, RNA-seq and RNC-seq were performed on HFD group and HB group mice liver. The identification and quantification information on transcriptome and translatome were given in Table S1−2. Principal component analysis shows that there is a high correlation between mRNA/RNC-mRNA abundance among the two biological repeats of each group, which indicates the reliable reproducibility of our analysis. More importantly, the difference obtained by RNC-seq is much larger than the difference obtained by RNA-seq between HFD group and HB group, which demonstrates that the translatome can reflect the difference between treatments better than the transcriptome (Figure 2C). About 16,000 genes were identified by RNA-seq and about 10,000 genes were identified by RNC-seq in HFD and HB groups (Figure 2D). When RNA-seq is compared with RNC-seq dataset, the majority of genes overlap (Figure 2D), which implies that most mRNAs have entered the translation process. The abundance of RNC-mRNAs in HFD group and HB group have a high correlation with mRNA ($R^2 = 0.5918$ and 0.4751, $p < 0.001$; Figure 2E), which suggests that the transcriptome and translatome can be combined for analysis. For single transcription level or single translation level, the gene expression abundance of HFD

group is highly correlated with that of HB group (R^2 = 0.8235 and 0.7271, $p < 0.001$; Figure S1A). The abundance distributions of RNC-mRNAs in HFD group and HB group are approximately lognormal (Figure 2F). Similar distributions are observed when it comes to the abundance distributions of mRNAs (Figures S1B).

Differential Transcriptome and Translatome Regulations in HFD and HB group mice livers

In order to identify the crucial functional genes related to phenotype, transcriptional and translational differentially expressed genes (DEGs) were screened by edge R method, respectively, with thresholds of |log2 (Fold Change) | > 1 and FDR < 0.01 for transcriptional DEGs; |log2 (Fold Change) | > 1 and FDR < 0.05 for translational DEGs. Overall, 1004 up-regulated and 882 down-regulated DEGs at the transcriptional level and 143 up-regulated and 181 down-regulated DEGs at the translational level were identified (Figure 3A). Figure 3B and 3C show the volcano plots of the fold changes for all the genes at transcriptional and translational levels. Gene ontology (GO) and Kyoto Encyclopedia of Genes and Genomes (KEGG) were analyzed with these transcriptional and translational DEGs. Several significant GO terms (classic Fisher <0.05) and KEGG pathways ($p < 0.05$) (Figure 3D and 3E) were obtained. In GO analysis, transcriptional and translational DEGs were enriched into biological processes such as lipid metabolism process, oxo acid metabolism process,

carboxylic acid metabolism process. In KEGG analysis, transcriptional and translational DEGs were enriched into pathways, such as non-alcoholic fatty liver disease (NAFLD), fatty acid metabolism, fatty acid degradation, fatty acid biosynthesis, fatty acid elongation. translational DEGs were directly enriched on Non-alcoholic fatty liver disease (NAFLD) pathway as expected.

Further study on the distribution of translational DEGs on chromosome — the number of translational DEGs carried by chromosome is standardized according to the length of each chromosome — shows that there is a significant enrichment on chromosome 11. As a result, GO annotation was made on the translational DEGs on chromosome 11. GO analysis shows that these genes were mainly related to the biosynthesis of ether lipid, glycerol ether and ether (Figure 4A). This indicates that betaine has more influence on genes on chromosome 11, and most of them are related to lipid metabolism. However, why so many translational DEGs are enriched on chromosome 11 needs further study.

Interestingly, it is found that some genes have different expression regulations at transcriptome and translatome levels. There are 88 genes shared by transcriptional and translational DEGs, but the rest are different (Figure 4B), which indicates that transcriptional regulation and translational regulation may be relatively independent. Similarly, in GO analysis, only 418 biological processes (BP) overlap between

transcriptional and translational DEGs (Figure 4C). In KEGG pathway analysis, only 20 significant enrichment pathways are shared by transcriptional and translational DEGs (Figure 4D). For example, compared with HFD group, *Anxa6* is shown to be up-regulated at mRNA level and down-regulated at RNC-mRNA level in HB group (Figure 4E). Another example shows the opposite situation, in which the mRNA level of *Upf3b* has decreased and the RNC-mRNA level has increased (Figure 4F). These results imply that transcriptional regulation and translational regulation play relatively independent roles in gene expression regulation.

HB-feeding Generates Increased TR

Translation ratio (TR) indicates the proportion of mRNA entering the translation process, which is also called translation initiation efficiency. TR value is the quotient of RNC-mRNA abundance and mRNA abundance. The mean mRNA abundance of HB group is slightly lower than that of HFD group (log2 mean mRNA RPKM of HFD = 1.368 and log2 mean mRNA RPKM of HB=0.9136, $p < 0.0001$; Figure 5A), the mean RNC-mRNA abundance in HB group is slightly higher than that in HFD group (log2 mean RNC-mRNA RPKM of HFD = 3.103 and log2 mean mRNA RPKM of HB =3.285, $p < 0.0001$; Figure 5A). Average TR of HB group is slightly higher than that of HFD group (log2 average TR of HFD=-0.1127, log2 average TR of HB = 0.1975, $p<0.0001$; Figure 5B). Similarly, for TR, the ratio of genes with higher TRs (log2 TR ≥ 1) in HB group is higher than

that in HFD group (Figure 5C). In addition, compared with HFD group, HB group has 767 differentially up-regulated TRs genes (DU-TR; log2 fold change>1, p<0.05), and 296 differentially down-regulated TRs genes (DD-TR; log2 fold change<-1, p<0.05). The genes corresponding to differentially up-regulated TR far exceed those differentially down-regulated (Figure 5D). All these results show that the translation ratio of HB group has increased.

Next, GO and KEGG enrichment analysis of differentially regulated TRs genes was conducted, and GO results show that it is related to translation, ribosome, ribosomal subunit and rRNA binding (classic Fisher <0.01; Figure S2A); KEGG results show that it is related to Ribosome and RNA transport ($p < 0.05$; Figure S2B). These results suggest that betaine may be involved in the regulation of lipid metabolism by affecting the mRNA translation process.

The Relationship Between TR and mRNA/RNC-mRNA Abundance

Effort was made to explore whether the abundance of mRNA and RNC-mRNA and the length of mRNA would affect TR. After statistical analysis, it is found that TR is weakly correlated with mRNA or RNC-mRNA abundance in HFD group and HB group (respectively,R^2=0.1537 and 0.0357, Figure S2C; R^2=0.1976 and 0.1431, Figure S2D； both p<0.001). TR has no high correlation with mRNA length in either HFD group or HB group (R^2 =0.0046 and 0.0007 respectively; Figure S2E). In the same way,

fold changes of TRs (HB/HFD) are still not highly correlated with mRNA length (R^2=0.0104；; Figure S2F). This indicates that the abundance of mRNA and RNC-mRNA and the length of mRNA have little contribution to translation regulation.

Distinct Nucleotide Preferences Between the Genes with Differentially up- and down-regulated TRs

The Kozak sequence[38], defined as 'GCCGCCRCCAUG'(R = A or G), plays a pivotal role in translation initiation, especially the 'G 'at the -6 position and the 'R' at the -3 position in the sequence (the 'A' of 'AUG' is at the 0 position)[39-41]. It is speculated that the Kozak sequence may affect the regulation of mRNA TRs. Therefore, the most significantly enriched motifs from HOMER (Hypergeometric Optimization of Motif Enrichment) de novo motif analysis were executed. A calculation was made regarding the probabilities of nucleotides around 'AUG' start codons of genes with differentially regulated TRs (DRTRs). In the present study, the differentially regulated TR genes with fold change>2 and *p* value < 0.05 were identified as DRTRs. A total of 296 differentially up-regulated genes and 767 differentially down-regulated genes were screened (Figure 5D). In the genes with non-DRTRs, there is a Kozak sequence with high probability near the start codon (Figure 5E). Common sequences are common among genes with DU- and DD-TRs, especially those with DU-TRs (Figure 5E). However, DD-TRs have some variations. For example,

the base at -9 changed from "G" to "U"; the base at -7 changed from "C" to "U"; and the base at -6 changed from "G" to "A". In other words, it is due to the effects of betaine on translation level regulation that there are more differentially up-regulated TR genes than differentially down-regulated TR genes (Figure 5D), and that the average TR value of HB is higher than HFD group (Figure 5B). More specifically, nucleotides at positions -9, -7 and -6 in Kozak sequence region attached to start codon change from "GC" to "AU" (Figure 5E), which may affect the process of mRNA translation.

Relationship Between Translational Regulation and Transcriptional Regulation

TR value represents the ratio of mRNA entering translation initiation, then the differential expression of RNC-mRNA abundance represents the result of gene regulation at transcription level and translation initiation level. Next, efforts were made to explore whether transcriptome regulation and translation initiation will affect the expression regulation of RNC-mRNA. As shown in Figure 6A, the genes were divided into nine quadrants according to the relationship between the fold change of mRNA at the transcription level and the fold change of TR at the translation initiation level. It is noticed that in e quadrant (-1<log2 fold change of mRNA<1, -1 < log2 fold change of TR < 1), there is no differential regulation of transcriptome and TR, and only a few DE RNC-mRNAs fall in quadrant e.

In other words, the vast majority of DE RNC-mRNAs fall into the quadrant of transcriptome differential regulation or TR differential regulation. This indicates that transcription regulation and translation initiation work together to change the abundance of RNC-mRNAs.

As mentioned above, the correlation between TR and mRNA abundance in HB group and HFD group is rather weak (Figure S2C). However, as shown in Figure 6A, there is a certain negative correlation between fold change of mRNA and TR ($R2=0.1975$, slope=-0.8258, $p<0.001$). The fold changes of mRNA and TR corresponding to differentially up-regulated and differentially down-regulated RNC-mRNA also have a certain negative correlation ($R2=0.1176$ and 0.3515, respectively; $p<0.001$). In other words, the fold change of TR will decrease with the increase of fold change of mRNA. To verify the negative correlation between fold change of mRNA and fold change of TR，the average fold change value of TR corresponding to up- and down- differentially expressed mRNA was calculated. The mean value of log2 fold change of TR for down-regulated mRNAs is greater than the mean value of log2 fold change of TR for up-regulated mRNAs (the mean value of log2 fold change of TR for up-regulated mRNAs =-1.113; the mean value of log2 fold change of TR for down-regulated mRNAs =1.479, $p<0.001$; Figure 6B). In the same way, for the majority of genes with DU-TRs and DD-TRs, opposite effects of transcriptional (Figure 6C). A more in-depth study was administered, where the abundance of mRNA

was divided into three levels according to the size of RPKM. Calculations were made on the TR values of all transcripts, non-differentially regulated transcripts, up-regulated transcripts and down-regulated transcripts in high, medium and low mRNA expression levels respectively. The results show that the TR values of genes with differentially down-regulated transcription levels are always higher than those with differentially up-regulated transcription levels, and the difference will be more significant with the increase of mRNA expression level in HFD group (Figure 6D). These results indicate that the transcriptional regulation and translation initiation regulation of most genes are opposite when HB alleviates HFD-induced liver fat deposition in mice.

Selection and Verification of Potential Functional Genes

The RNA-seq and RNC-seq data of the NFD group obtained in our previous study were used to screen candidate functional genes[30]. According to the threshold | log2 fold change | > 1 and FDR < 0.01, 31 transcriptional DEGs and 106 translational DEGs respectively were selected in the comparison of HFD group and NFD group. As mentioned in Figure 3A, 1886 transcriptional DEGs and 324 translational DEGs were selected in the comparison of HB group and HFD group. For translational DEGs, only 8 genes are shared by different genes in HFD group compared with NFD group and HB group compared with HFD group (left in Figure 7A). For transcriptional DEGs, only 7 genes are shared by the different

genes in HFD group compared with NFD group and HB group compared with HFD (right in Figure 7A). Furthermore, for HB group compared with HFD group and HFD group Compared with NFD group, the heat maps show the log2 fold changes of 8 translational DEGs and the log2 fold changes of 7 transcriptional DEGs (Figure 7B). Finally, the literatures on the function of these 15 candidate genes were searched. Except *Egfr*, *Cxcl1* and *Gpc1*(glypican 1), other genes have been claimed to be related to lipid metabolism. Then, predictions can be made that these three genes also have a certain role in lipid metabolism. Due to the high expression abundance of *Gpc1* (RPKM>10), *Gpc1* was selected to subsequent functional verification. In HepG2 cells, the expression of *Gpc1* in OA/PA+Betaine group is significantly higher than that in OA/PA group (Figure 7C left), which is consistent with RNA-seq and RNC-seq sequencing results (Figure 7C right). *Gpc1* was knocked down and its mRNA expression was inhibited by about 30% (Figure 7D). Accordingly, intracellular TG level in GPC1-knockdown cells has increased by about 61% (Figure 7E left) and extracellular TG level has increased by about 6% (Figure 7E right). This provides a preliminary verification of this hypothesis (*Gpc1* inhibits TG accumulation) and provides a new potential target gene for the treatment of NAFLD.

Discussion

NAFLD is a disorder of lipid metabolism in the liver. Excessive fat

accumulation in the liver can lead to local and systemic problems. At present, there is no effective method to control NAFLD. There is increasing evidence that adding betaine to food is an effective strategy to improve lipid metabolism in the liver. It has been reported that mitochondria are the main site of cellular energy metabolism and play a fundamental role in fatty acid oxidation. Betaine can increase mitochondrial content and ATP level[23]. The beneficial effects of betaine on NAFLD are associated with the reduction of hepatic oxidative stress, inflammation and apoptosis, and the enhancement of Akt/mTOR signaling and autophagy[42]. This study also proves that the TG level in the liver of mice in the HB group has significantly decreased compared with that in the HFD group (Figure 2A and B).

Betaine, as a natural methyl donor, has certain influence on the m^6A methylation apparent modification of mRNA. It has been reported that m^6A readers may cause different downstream effects by recognizing m^6A apparent modification[43-45]. The binding of YTHDF2 protein to m^6A site is related to shortening the half-life of mRNA, and can maintain the m^6A modification of 5'UTR region, thus promoting nonclassical mRNA translation. Therefore, it is worthy to study the effect of betaine on mRNA translation. Translatome, as a new technology of omics research in recent years, may provide important information on many biological problems for further research. It has been reported that RNC-seq can detect lncRNA[46-

48], circRNA[49-51] and pri-miRNA[52] which encode polypeptide. These RNA molecules, considered as "non-coding" in the past, contain one or more small open reading frames (small ORFs), which can be translated into small peptides with less than 100 amino acids. Therefore, RNC-seq was conducted for the phenotype that betaine can alleviate hepatic steatosis. In transcriptome and translatome analysis, it is found that translation level can reflect the difference between different treatments more significantly compared with transcription level (Figure 2C). In GO and KEGG enrichment analysis, differentially expressed genes at the transcription and translation level are significantly enriched in biological processes and pathways related phenotype (Figure 3D and E), indicating that betaine participates in both transcription and translation regulation in the process of fat accumulation. In particular, the differentially expressed RNC-mRNA is directly enriched in NAFLD pathway by KEGG analysis, which means that betaine plays an important role in the translation regulation of NAFLD. Interestingly, there are 88 common genes at the intersection of differential expressed mRNA and RNC mRNA (Figure 4B). Among them, there are many genes with opposite regulation at transcriptional and translational levels, as shown in the two examples in Figure 4E and F. This suggests that transcriptional regulation and translation regulation may be independent from each other. When studying the expression abundance of the coding gene, it is really about examining the end product (protein) of the central

principle, rather than the intermediate mRNA. However, due to the convenience of RNA-seq detection and the weak sensitivity of protein mass spectrometry detection, RNA-seq is the most widely used method. This means that in this case we treat the transcriptional abundance of the gene as a functional product (protein abundance). Obviously, this alternative approach has a certain bias. RNC-Seq has the advantages of high throughput and sensitivity of RNA-Seq, as well as good correlation with actual protein abundance, so it can be used as a new analytical method to solve biomedical problems.

As for the study on translation initiation efficiency, the results show that betaine treatment can improve the translation ratio of mRNA on the overall level (Figure 5B and C), suggesting that betaine may affect the entry process of mRNA into translation, thereby affecting the accumulation of fat in the liver. In order to further study translation initiation, Homer motif analysis was made. The Kozak sequence is considered to be an important sequence to identify the initiation codon effectively. It was speculated that the nucleotide preference of the corresponding position of Kozak sequence of DD-TRs mRNA would change, and the analysis results are in line with the expectation. The nucleotides at -9, -7, -6 near the initial codon 'AUG' of DD-TR corresponding mRNA are different from the standard Kozak sequences. Inversely, the nucleotide preference remains unchanged in ND-TR and DD-TR corresponding mRNA. In other words, the nucleotides at

positions -9, -7 and -6 in Kozak sequence region attached to start codon changed from "GC" to "AU". The above results suggest that betaine does affect the process of some mRNA into translation, thus alleviating NAFLD. The relationship between the abundance of mRNA expression and TR was analyzed. The results show no significant correlation, indicating that the expression level of a mRNA has nothing to do with the efficiency of entering translation initiation (Figure S2A). Furthermore, the relationship between the length of mRNA and TR was analyzed, and the results shows that the length of mRNA is not related to the translation ratio (Figure S2C). Finally, through the joint analysis of translatome and transcriptome, 15 candidate genes (*Cyp4a14*, *Plin4*, *Cyp2b9*, *Egfr*, *Scd1*, *Fasn*, *Elovl6*, *Me1*, *Cxcl1*, *Gpc1*, *Apoa4*, *Mogat1*, *Hcn3*, *Ntrk2*, *Pnpla3*) were screened. The literatures on the function of these 15 candidate genes were searched. Except *Egfr*, *Cxcl1* and *Gpc1*, other genes have been claimed to be related to lipid metabolism. Then, predictions can be made that these three genes also have a certain role in lipid metabolism. Further, *Gpc1* inhibiting TG accumulation was verified.

Conclusion

The results that include triglyceride measurement and oil red O staining demonstrated that betaine improved HFD-induced hepatic steatosis. Through the integrative application of hepatic transcriptome and translatome, the pharmacological mechanism of betaine and a potential

therapeutic effect were achieved. Based on our multiomics analysis, 1886 differentially expressed genes at the transcriptome and 324 differentially expressed genes at the translatome were revealed for their potential roles in HFD-induced hepatic steatosis, which mainly enriched in non-alcoholic fatty liver disease pathway, fatty acid metabolism, fatty acid degradation, fatty acid biosynthesis, fatty acid elongation. Further screening and verification showed that *Gpc1* is a novel functional gene, which could regulate lipid metabolism in liver. This study showed that the integration of transcriptome and translatome is a promising tool in exploring the anti-NAFLD effects of betaine and providing a clue for understanding the molecular mechanisms.

Ethics approval and consent to participate: The study was conducted according to the guidelines of the Declaration of Helsinki, and approved by the Animal Protection and Utilization Committee of Guangxi university (No. GXU2019-063).

Consent for publication

Not applicable

Availability of data and materials

All data generated or analysed during this study are included in this published article and its supplementary information files.

Competing interests

The authors have no competing interests to declare.

Funding

This work was funded by the National Key R&D Program of China (2018YFD0500402), Guangxi Science Foundation for Distinguished Young Scholars (2020JJG130006), Guangxi Science and Technology Base and Talents Project (GuikeAD18281085), Guangxi Natural Science Foundation (2019GXNSFDA245029), Innovation Project of Guangxi Graduate Education (YCBZ2020003), Guangxi Hundred-Talent Program, State Key Laboratory for Conservation and Utilization of Subtropical Agrobioresources (SKLCUSA-a202006), Training Project of High-level Professional and Technical Talents of Guangxi University.

Authors' contributions

All authors have contributed substantially to the work reported. Tengda Huang, Jingsu Yu, and Lei Zhou conceived the project and design the protocol; Tengda Huang, Lin Yu, Siqi Liu, Mengtin Jia, Peng Wang, Tian Wu, Yurou Zhang, and Ziyi Song performed the experiments; Tengda Huang, Weiwei Miao and Yixing Li performed the data analysis; Tengda Huang, Zupeng Luo, Haojie Zhang and Yixing Li wrote the manuscript. All authors read and approved the final manuscript.

Acknowledgments: We would like to thank Shenzhen Chi-Biotech Co. Ltd for invaluable support on the RNC-mRNA extraction experiment in terms of method optimization and for their assistance on RNC-mRNA data analysis.

Abbreviations used: NFD, normal-fat diet; HFD, high-fat diet; HB, HFD+ betaine; TG, triglyceride; RNC-mRNA, mRNA bound to ribosome-nascent chain complex; RNC-seq, RNC-mRNA sequencing; RNA-seq, mRNA sequencing; RPKM, reads per kilo base per million reads; DEGs, differentially expressed genes; DE mRNA, differentially expressed mRNA; DE RNC-mRNA, differentially expressed RNC-mRNA; TR, translation ratio; DR TR, differentially regulated TR; DU-TR, differentially up-regulated TR; DD-TR, differentially down-regulated TR; GO, Gene Ontology; KEGG, Kyoto Encyclopedia of Genes and Genomes; NAFLD, non-alcoholic fatty liver disease; FDR, false discovery rates; vs., versus;

Figure legends

Figure 1. Overview of experimental strategy

Figure 2. Phenotypes of experimental treatment and characteristics of data obtained from RNA-seq and RNC-seq

NFD: normal-fat diet; HFD: high-fat diet; HB: HFD + betaine. (A) Triglyceride (TG) concentrations in the mouse livers (n = 3). Error bars represent the standard deviation. **p<0.01, ***p < 0.001, one-way analysis of variance（ANOVA）. (B) Oil red O staining of the liver sections. (C) Principal component analysis (PCA): For HFD group and HB group, the relationships between two biological repeats obtained by RNA-seq and RNC-seq. Each point represents a sample of HFD group or HB group. (D) Venn diagrams of genes identified by RNA-seq and RNC-seq in HFD and

HB groups. (E) Correlation between mRNA and RNC-mRNA abundance in the HFD and HB groups. Each point represents a gene sequenced by RNA-seq and RNC-seq. (F) Distribution of the RNC-mRNA abundance in HFD and HB groups. Genes were classified based on their rounded log2 RPKM abundance. Each bar represents the gene count detected by RNC-seq in each category.

Figure 3. Analysis of differentially expressed genes at transcription level and translation level

(A) Statistics of differentially up- and down-expressed gene in transcriptome and translatome. (B) Volcano map: | log2 fold change of mRNA | > 1, FDR < 0.01 as the threshold value, the differentially expressed mRNAs were screened. (C) Volcano map: | log2 fold change of mRNA | > 1, FDR < 0.05 as the threshold value, the differentially expressed RNC-mRNA were screened. (D) Pyramid figure： The transcriptional and translational DEGs were analyzed by Gene Ontology (GO), and their TOP10 biological processes were ranked by -log10 (classic Fisher), The enrichment p-value of the terms ID used Fisher's exact test. (E) The transcriptional and translational DEGs were analyzed by Kyoto Encyclopedia of Genes and Genomes (KEGG), and their TOP20 pathways were ranked by -log10 (p-value).

Figure 4. Further analysis of DE mRNA and DE RNC-mRNA

(A) Left: Distribution of translational DEGs across chromosomes. A heat

map showing relative coverage of translational DEGs in each chromosome standardized according to the length of each chromosome. Right: significantly enriched GO biological processes (BPs) by translational DEGs in chromosome 11. (B) Venn diagram of differentially expressed mRNAs (DE mRNAs) and RNC-mRNAs (DE RNC-mRNAs). (C) Venn diagrams of significantly enriched GO BPs by DE mRNAs and DE RNC-mRNAs. (D) Venn diagrams of significantly enriched KEGG pathways by DE mRNAs and DE RNC-mRNAs. (E and F) IGV analysis at transcription level and translation level. Two examples showing the different direction of regulation between transcriptome and translatome. Two biological replicate tracks were overlaid into one. (E) *Anxa6* was up-regulated at the mRNA level but down-regulated at the RNC-mRNA level. (F) While *Upf3b* was down-regulated at the mRNA level but up-regulated at the RNC-mRNA level.

Figure 5. Translation ratio analysis

(A) Violin plot of mean abundance in mRNA and RNC-mRNA of HFD group and HB group (The gene abundance is represented by $\log_2$ RPKM. ****$p < 0.0001$, one-way analysis of variance（ANOVA）). (B) Violin plot of TR in HFD and HB groups. ****$p < 0.0001$, student's t-test. (C) Relative TR distribution. Genes were classified based on their rounded log2 TR values. For HFD or HB groups in each category, every bar represents the percentage of the gene counts in this group to the total gene count. (D)

Volcano map: | log2 fold change of mRNA | > 1, p-value < 0.01 as the threshold value, the differentially regulated TRs were screened. (E) Sequence composition between TR-differentially-up and -down-regulated genes around the AUG start codon.

Figure 6. Correlation between transcriptional and translational regulation, in the

HB group versus HFD group

(A) Correlation of the fold change of mRNA abundance and TRs. Nine squares indicate nine corresponding categories. (B) Relative fold change of TR distribution of differentially regulated mRNAs. ***p < 0.001, student's t-test. (C) mRNA fold change value distribution in genes with differentially regulated TRs. ***p < 0.001, student's t-test. (D) Distribution of TR values corresponding to transcripts with different expression levels. *p < 0.05, **p < 0.01, ****p < 0.0001, one-way analysis of variance （ANOVA）.

Figure 7. Functional gene screening and functional verification

(A) Left: Venn diagrams: Intersection of translational DEGs in HFD vs. NFD and translational DEGs in HB vs. HFD. Right: Venn diagrams: Intersection of transcriptional DEGs in HFD vs. NFD and transcriptional DEGs in HB vs. HFD. (B) List of screened candidate genes. In comparisons of HFD vs. NFD and HB vs. HFD, genes with different regulation were selected, both at the transcriptome and translatome. (C)

Left: Relative level of *Gpc1* mRNA expression in HepG2 cells in the OA/PA and OA/PA + Betaine group (n = 4). Error bars represent the standard error of the mean. ***p < 0.001, the Student's *t*-test. Right: IGV analysis at transcription level and translation level, *Gpc1* was up-regulated at the transcriptome and translatome. (D) Relative level of *Gpc1* mRNA expression in HepG2 cells transfected with siRNA, compared to the controls (NC) (n = 4). Error bars represent the standard error of the mean. ***p < 0.001, the Student's *t*-test. (E) Intracellular and extracellular TG concentration in *Gpc1* knockdown cells (n = 4). Error bars represent the standard error of the mean. *p < 0.05, **p < 0.01, the Student's *t*-test.

Figure S1. mRNA data characteristics

(A) Correlation between HFD abundance and HB abundance in single RNA-seq and RNC-seq. Each point represents a gene sequenced by RNA-seq or RNC-seq. (B) Distribution of the mRNA abundance in HFD and HB groups. Genes were classified based on their rounded log2 RPKM abundance. Each bar represents the gene count detected by RNA-seq in each category.

Figure S2. TR GO and KEGG analysis

(A and B) Differentially expressed TR analysis of HB vs. HFD. (A) Top 10 significantly enriched GO biological processes, cellular component and molecular function terms. (B)Significantly enriched KEGG pathways. (C) Correlation of mRNA abundance and TR in HFD and HB groups,

respectively. (D) Correlation of RNC-mRNA abundance and TR in HFD and HB groups, respectively. (E) Correlation of mRNA max length and TR in HFD and HB groups, respectively. (F) Correlation of mRNA max length and fold change of TR in HFD and HB groups, respectively.

References

1. Yki-Jarvinen, H. Non-alcoholic fatty liver disease as a cause and a consequence of metabolic syndrome. *Lancet Diabetes Endocrinol* **2014**, 2, 901-910, doi:10.1016/S2213-8587(14)70032-4.
2. Bazick, J.; Donithan, M.; Neuschwander-Tetri, B.A.; Kleiner, D.; Brunt, E.M.; Wilson, L.; Doo, E.; Lavine, J.; Tonascia, J.; Loomba, R. Clinical Model for NASH and Advanced Fibrosis in Adult Patients with Diabetes and NAFLD: Guidelines for Referral in NAFLD. *Diabetes Care* **2015**, 38, 1347-1355, doi:10.2337/dc14-1239.
3. Sumida, Y.; Yoneda, M.; Tokushige, K.; Kawanaka, M.; Fujii, H.; Yoneda, M.; Imajo, K.; Takahashi, H.; Eguchi, Y.; Ono, M., et al. Antidiabetic Therapy in the Treatment of Nonalcoholic Steatohepatitis. *Int J Mol Sci* **2020**, 21, doi:10.3390/ijms21061907.
4. Green, C.J.; Hodson, L. The influence of dietary fat on liver fat accumulation. *Nutrients* **2014**, 6, 5018-5033, doi:10.3390/nu6115018.
5. Jennison, E.; Patel, J.; Scorletti, E.; Byrne, C.D. Diagnosis and management of non-alcoholic fatty liver disease. *Postgrad Med J* **2019**, 95, 314-322, doi:10.1136/postgradmedj-2018-136316.
6. Paul, S.; Davis, A.M. Diagnosis and Management of Nonalcoholic Fatty Liver Disease. *JAMA* **2018**, 320, 2474-2475, doi:10.1001/jama.2018.17365.

7. Petta, S.; Ciresi, A.; Bianco, J.; Geraci, V.; Boemi, R.; Galvano, L.; Magliozzo, F.; Merlino, G.; Craxi, A.; Giordano, C. Insulin resistance and hyperandrogenism drive steatosis and fibrosis risk in young females with PCOS. *Plos One* **2017**, 12, e186136, doi: 10.1371/journal.pone.0186136.
8. Rial, S.A.; Ravaut, G.; Malaret, T.B.; Bergeron, K.F.; Mounier, C. Hexanoic, Octanoic and Decanoic Acids Promote Basal and Insulin-Induced Phosphorylation of the Akt-mTOR Axis and a Balanced Lipid Metabolism in the HepG2 Hepatoma Cell Line. *Molecules* **2018**, 23, doi:10.3390/molecules23092315.
9. Herath, H.; Kodikara, I.; Weerarathna, T.P.; Liyanage, G. Prevalence and associations of non-alcoholic fatty liver disease (NAFLD) in Sri Lankan patients with type 2 diabetes: A single center study. *Diabetes Metab Syndr* **2019**, 13, 246-250, doi: 10.1016/j.dsx.2018.09.002.
10. Brouwers, M.; Simons, N.; Stehouwer, C.; Isaacs, A. Non-alcoholic fatty liver disease and cardiovascular disease: assessing the evidence for causality. *Diabetologia* **2020**, 63, 253-260, doi:10.1007/s00125-019-05024-3.
11. Clarke, J.D.; Dzierlenga, A.L.; Nelson, N.R.; Li, H.; Werts, S.; Goedken, M.J.; Cherrington, N.J. Mechanism of Altered Metformin Distribution in Nonalcoholic Steatohepatitis. *Diabetes* **2015**, 64, 3305-3313, doi:10.2337/db14-1947.
12. Zhou, X.; Fouda, S.; Li, D.; Zhang, K.; Ye, J.M. Involvement of the Autophagy-ER Stress Axis in High Fat/Carbohydrate Diet-Induced Nonalcoholic Fatty Liver Disease. *Nutrients* **2020**, 12, doi:10.3390/nu12092626.
13. Zhang, Q.; Guo, J.H.; Zhou, L.S.; Dong, H. [Research progress of non-alcoholic fatty

liver disease in postmenopausal women]. *Zhonghua Gan Zang Bing Za Zhi* **2020**, 28, 629-632, doi:10.3760/cma.j.cn501113-20200525-00270.

14. Komine, S.; Akiyama, K.; Warabi, E.; Oh, S.; Kuga, K.; Ishige, K.; Togashi, S.; Yanagawa, T.; Shoda, J. Exercise training enhances in vivo clearance of endotoxin and attenuates inflammatory responses by potentiating Kupffer cell phagocytosis. *Sci Rep* **2017**, 7, 11977, doi:10.1038/s41598-017-12358-8.
15. Fiorito, S.; Preziuso, F.; Epifano, F.; Scotti, L.; Bucciarelli, T.; Taddeo, V.A.; Genovese, S. Novel biologically active principles from spinach, goji and quinoa. *Food Chem* **2019**, 276, 262-265, doi: 10.1016/j.foodchem.2018.10.018.
16. Wei, F.; Shi, Z.; Wan, R.; Li, Y.; Wang, Y.; An, W.; Qin, K.; Cao, Y.; Chen, X.; Wang, X., et al. Impact of phosphorus fertilizer level on the yield and metabolome of goji fruit. *Sci Rep* **2020**, 10, 14656, doi:10.1038/s41598-020-71492-y.
17. Craig, S.A. Betaine in human nutrition. *Am J Clin Nutr* **2004**, 80, 539-549, doi:10.1093/ajcn/80.3.539.
18. Zhao, G.; He, F.; Wu, C.; Li, P.; Li, N.; Deng, J.; Zhu, G.; Ren, W.; Peng, Y. Betaine in Inflammation: Mechanistic Aspects and Applications. *Front Immunol* **2018**, 9, 1070, doi:10.3389/fimmu.2018.01070.
19. Chen, W.; Zhang, X.; Xu, M.; Jiang, L.; Zhou, M.; Liu, W.; Chen, Z.; Wang, Y.; Zou, Q.; Wang, L. Betaine prevented high-fat diet-induced NAFLD by regulating the FGF10/AMPK signaling pathway in ApoE(-/-) mice. *Eur J Nutr* **2020**, doi:10.1007/s00394-020-02362-6.
20. Kathirvel, E.; Morgan, K.; Nandgiri, G.; Sandoval, B.C.; Caudill, M.A.; Bottiglieri, T.;

French, S.W.; Morgan, T.R. Betaine improves nonalcoholic fatty liver and associated hepatic insulin resistance: a potential mechanism for hepatoprotection by betaine. *Am J Physiol Gastrointest Liver Physiol* **2010**, 299, G1068-G1077, doi:10.1152/ajpgi.00249.2010.

21. Hu, Y.; Sun, Q.; Liu, J.; Jia, Y.; Cai, D.; Idriss, A.A.; Omer, N.A.; Zhao, R. In ovo injection of betaine alleviates corticosterone-induced fatty liver in chickens through epigenetic modifications. *Sci Rep* **2017**, 7, 40251, doi:10.1038/srep40251.
22. Wang, L.J.; Zhang, H.W.; Zhou, J.Y.; Liu, Y.; Yang, Y.; Chen, X.L.; Zhu, C.H.; Zheng, R.D.; Ling, W.H.; Zhu, H.L. Betaine attenuates hepatic steatosis by reducing methylation of the MTTP promoter and elevating genomic methylation in mice fed a high-fat diet. *J Nutr Biochem* **2014**, 25, 329-336, doi: 10.1016/j.jnutbio.2013.11.007.
23. Zhang, L.; Qi, Y.; ALuo, Z.; Liu, S.; Zhang, Z.; Zhou, L. Betaine increases mitochondrial content and improves hepatic lipid metabolism. *Food Funct* **2019**, 10, 216-223, doi:10.1039/c8fo02004c.
24. Veskovic, M.; Labudovic-Borovic, M.; Mladenovic, D.; Jadzic, J.; Jorgacevic, B.; Vukicevic, D.; Vucevic, D.; Radosavljevic, T. Effect of Betaine Supplementation on Liver Tissue and Ultrastructural Changes in Methionine-Choline-Deficient Diet-Induced NAFLD. *Microsc Microanal* **2020**, 26, 997-1006, doi:10.1017/S1431927620024265.
25. Shapiro, J.A. Revisiting the central dogma in the 21st century. *Ann N Y Acad Sci* **2009**, 1178, 6-28, doi:10.1111/j.1749-6632.2009.04990. x.
26. Schwanhausser, B.; Busse, D.; Li, N.; Dittmar, G.; Schuchhardt, J.; Wolf, J.; Chen, W.;

Selbach, M. Global quantification of mammalian gene expression control. *Nature* **2011**, 473, 337-342, doi:10.1038/nature10098.

27. Halbeisen, R.E.; Gerber, A.P. Stress-dependent coordination of transcriptome and translatome in yeast. *Plos Biol* **2009**, 7, e1000105, doi: 10.1371/journal.pbio.1000105.
28. Payne, S.H. The utility of protein and mRNA correlation. *Trends Biochem Sci* **2015**, 40, 1-3, doi: 10.1016/j.tibs.2014.10.010.
29. Liu, M.; Ge, R.; Liu, W.; Liu, Q.; Xia, X.; Lai, M.; Liang, L.; Li, C.; Song, L.; Zhen, B., et al. Differential proteomics profiling identifies LDPs and biological functions in high-fat diet-induced fatty livers. *J Lipid Res* **2017**, 58, 681-694, doi:10.1194/jlr.M071407.
30. Luo, Z.; Hu, H.; Liu, S.; Zhang, Z.; Li, Y.; Zhou, L. Comprehensive analysis of the translatome reveals the relationship between the translational and transcriptional control in high fat diet-induced liver steatosis. *Rna Biol* **2020**, 1-12, doi:10.1080/15476286.2020.1827193.
31. Wang, T.; Cui, Y.; Jin, J.; Guo, J.; Wang, G.; Yin, X.; He, Q.Y.; Zhang, G. Translating mRNAs strongly correlate to proteins in a multivariate manner and their translation ratios are phenotype specific. *Nucleic Acids Res* **2013**, 41, 4743-4754, doi:10.1093/nar/gkt178.
32. Sales, R.C.; Medeiros, P.C.; Spreafico, F.; de Velasco, P.C.; Goncalves, F.; Martin-Hernandez, R.; Mantilla-Escalante, D.C.; Gil-Zamorano, J.; Peres, W.; de Souza, S., et al. Olive Oil, Palm Oil, and Hybrid Palm Oil Distinctly Modulate Liver Transcriptome and Induce NAFLD in Mice Fed a High-Fat Diet. *Int J Mol Sci* **2018**, 20,

doi:10.3390/ijms20010008.

33. Liu, S.; Yang, D.; Yu, L.; Aluo, Z.; Zhang, Z.; Qi, Y.; Li, Y.; Song, Z.; Xu, G.; Zhou, L. Effects of lycopene on skeletal muscle-fiber type and high-fat diet-induced oxidative stress. *J Nutr Biochem* **2021**, 87, 108523, doi: 10.1016/j.jnutbio.2020.108523.
34. Wang, L.; Chen, L.; Tan, Y.; Wei, J.; Chang, Y.; Jin, T.; Zhu, H. Betaine supplement alleviates hepatic triglyceride accumulation of apolipoprotein E deficient mice via reducing methylation of peroxisomal proliferator-activated receptor alpha promoter. *Lipids Health Dis* **2013**, 12, 34, doi:10.1186/1476-511X-12-34.
35. Xiao, C.L.; Mai, Z.B.; Lian, X.L.; Zhong, J.Y.; Jin, J.J.; He, Q.Y.; Zhang, G. FANSe2: a robust and cost-efficient alignment tool for quantitative next-generation sequencing applications. *Plos One* **2014**, 9, e94250, doi: 10.1371/journal.pone.0094250.
36. Mortazavi, A.; Williams, B.A.; McCue, K.; Schaeffer, L.; Wold, B. Mapping and quantifying mammalian transcriptomes by RNA-Seq. *Nat Methods* **2008**, 5, 621-628, doi:10.1038/nmeth.1226.
37. Robinson, M.D.; McCarthy, D.J.; Smyth, G.K. edgeR: a Bioconductor package for differential expression analysis of digital gene expression data. *Bioinformatics* **2010**, 26, 139-140, doi:10.1093/bioinformatics/btp616.
38. Hernandez, G.; Osnaya, V.G.; Perez-Martinez, X. Conservation and Variability of the AUG Initiation Codon Context in Eukaryotes. *Trends Biochem Sci* **2019**, 44, 1009-1021, doi: 10.1016/j.tibs.2019.07.001.
39. De Angioletti, M.; Lacerra, G.; Sabato, V.; Carestia, C. Beta+45 G --> C: a novel silent beta-thalassaemia mutation, the first in the Kozak sequence. *Br J Haematol* **2004**, 124,

224-231, doi:10.1046/j.1365-2141.2003.04754. x.

40. Kozak, M. An analysis of 5'-noncoding sequences from 699 vertebrate messenger RNAs. *Nucleic Acids Res* **1987**, 15, 8125-8148, doi:10.1093/nar/15.20.8125.
41. Kozak, M. Pushing the limits of the scanning mechanism for initiation of translation. *Gene* **2002**, 299, 1-34, doi:10.1016/s0378-1119(02)01056-9.
42. Veskovic, M.; Mladenovic, D.; Milenkovic, M.; Tosic, J.; Borozan, S.; Gopcevic, K.; Labudovic-Borovic, M.; Dragutinovic, V.; Vucevic, D.; Jorgacevic, B., et al. Betaine modulates oxidative stress, inflammation, apoptosis, autophagy, and Akt/mTOR signaling in methionine-choline deficiency-induced fatty liver disease. *Eur J Pharmacol* **2019**, 848, 39-48, doi: 10.1016/j.ejphar.2019.01.043.
43. Cao, G.; Li, H.B.; Yin, Z.; Flavell, R.A. Recent advances in dynamic m6A RNA modification. *Open Biol* **2016**, 6, 160003, doi:10.1098/rsob.160003.
44. Deng, X.; Su, R.; Weng, H.; Huang, H.; Li, Z.; Chen, J. RNA N (6)-methyladenosine modification in cancers: current status and perspectives. *Cell Res* **2018**, 28, 507-517, doi:10.1038/s41422-018-0034-6.
45. Zhong, J.; Cui, Y.; Guo, J.; Chen, Z.; Yang, L.; He, Q.Y.; Zhang, G.; Wang, T. Resolving chromosome-centric human proteome with translating mRNA analysis: a strategic demonstration. *J Proteome Res* **2014**, 13, 50-59, doi:10.1021/pr4007409.
46. Kondo, T.; Plaza, S.; Zanet, J.; Benrabah, E.; Valenti, P.; Hashimoto, Y.; Kobayashi, S.; Payre, F.; Kageyama, Y. Small peptides switch the transcriptional activity of Shavenbaby during Drosophila embryogenesis. *Science* **2010**, 329, 336-339, doi:10.1126/science.1188158.

47. Anderson, D.M.; Anderson, K.M.; Chang, C.L.; Makarewich, C.A.; Nelson, B.R.; McAnally, J.R.; Kasaragod, P.; Shelton, J.M.; Liou, J.; Bassel-Duby, R., et al. A micropeptide encoded by a putative long noncoding RNA regulates muscle performance. *Cell* **2015**, 160, 595-606, doi: 10.1016/j.cell.2015.01.009.

48. Magny, E.G.; Pueyo, J.I.; Pearl, F.M.; Cespedes, M.A.; Niven, J.E.; Bishop, S.A.; Couso, J.P. Conserved regulation of cardiac calcium uptake by peptides encoded in small open reading frames. *Science* **2013**, 341, 1116-1120, doi:10.1126/science.1238802.

49. Zhang, M.; Huang, N.; Yang, X.; Luo, J.; Yan, S.; Xiao, F.; Chen, W.; Gao, X.; Zhao, K.; Zhou, H., et al. A novel protein encoded by the circular form of the SHPRH gene suppresses glioma tumorigenesis. *Oncogene* **2018**, 37, 1805-1814, doi:10.1038/s41388-017-0019-9.

50. Zhang, M.; Zhao, K.; Xu, X.; Yang, Y.; Yan, S.; Wei, P.; Liu, H.; Xu, J.; Xiao, F.; Zhou, H., et al. A peptide encoded by circular form of LINC-PINT suppresses oncogenic transcriptional elongation in glioblastoma. *Nat Commun* **2018**, 9, 4475, doi:10.1038/s41467-018-06862-2.

51. Yang, Y.; Gao, X.; Zhang, M.; Yan, S.; Sun, C.; Xiao, F.; Huang, N.; Yang, X.; Zhao, K.; Zhou, H., et al. Novel Role of FBXW7 Circular RNA in Repressing Glioma Tumorigenesis. *J Natl Cancer Inst* **2018**, 110, doi:10.1093/jnci/djx166.

52. Lauressergues, D.; Couzigou, J.M.; Clemente, H.S.; Martinez, Y.; Dunand, C.; Becard, G.; Combier, J.P. Primary transcripts of microRNAs encode regulatory peptides. *Nature* **2015**, 520, 90-93, doi:10.1038/nature14346.

Figures

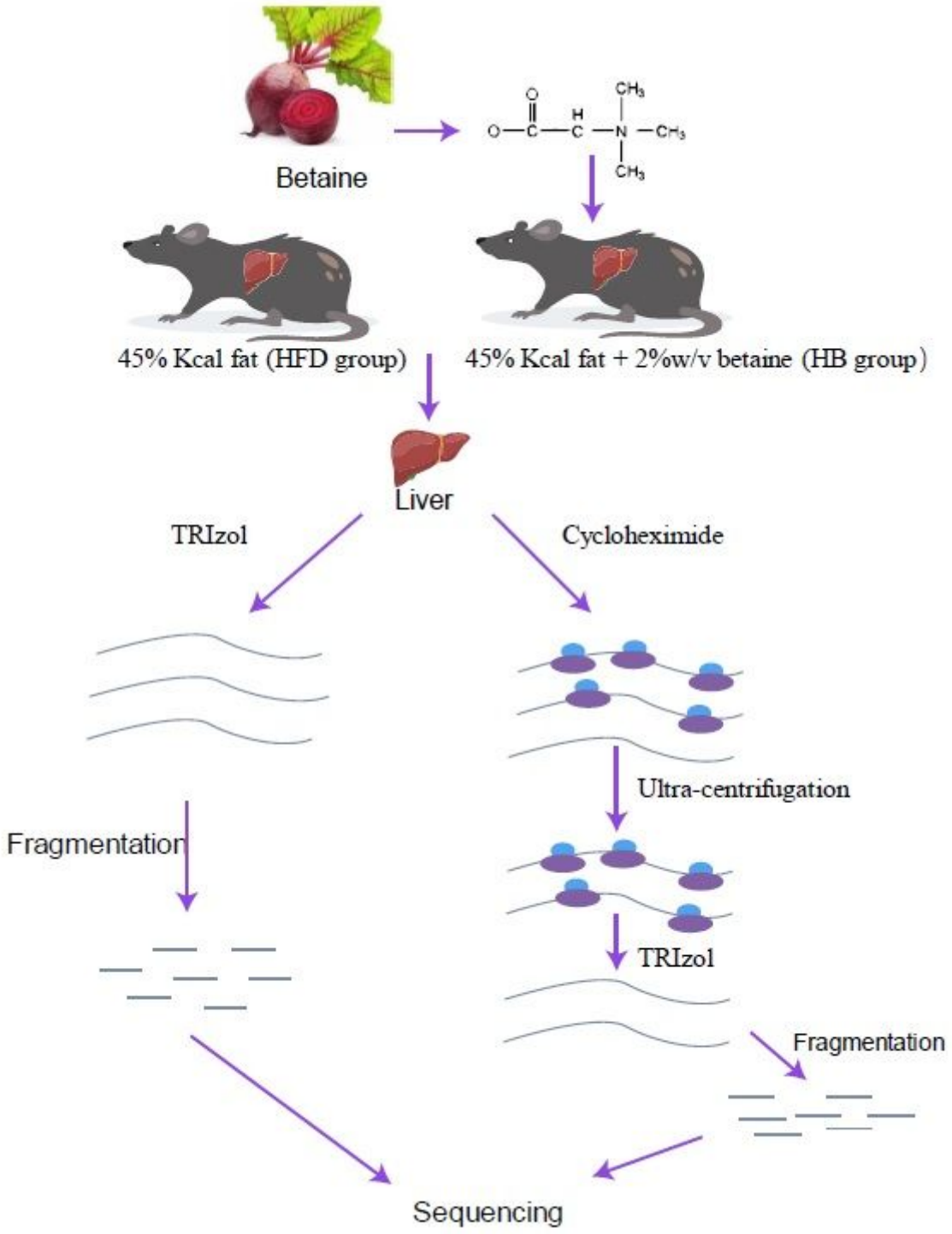

Figure 1

Overview of experimental strategy

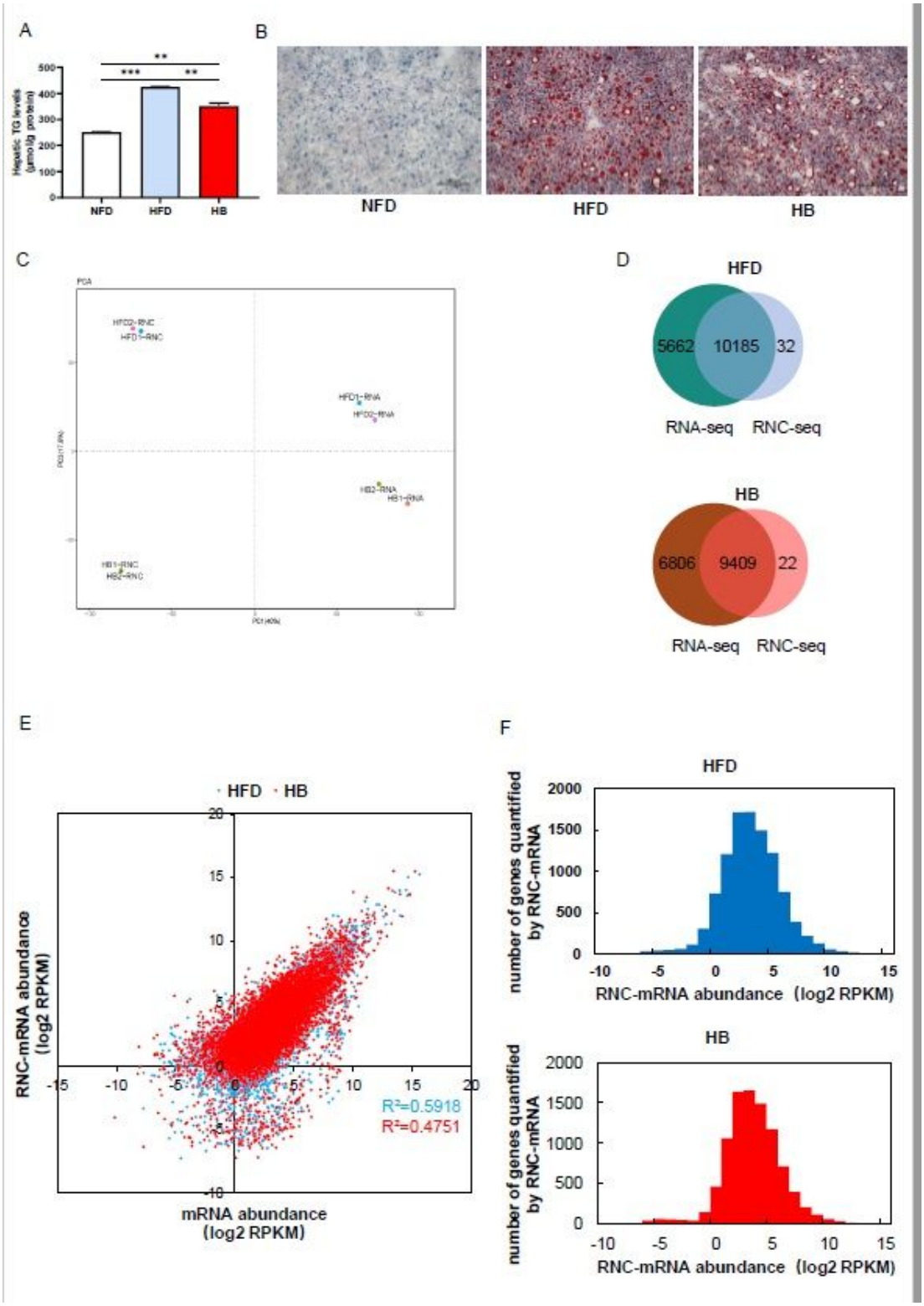

Figure 2

Phenotypes of experimental treatment and characteristics of data obtained from RNA-seq and RNC-seq NFD: normal-fat diet; HFD: high-fat diet; HB: HFD + betaine. (A) Triglyceride (TG) concentrations in the mouse livers (n = 3). Error bars represent the standard deviation. **p<0.01, ***p < 0.001, one-way analysis of variance ANOVA. (B) Oil red O staining of the liver sections. (C) Principal component analysis (PCA): For HFD group and HB group, the relationships between two biological repeats obtained by RNA-seq and

RNC-seq. Each point represents a sample of HFD group or HB group. (D) Venn diagrams of genes identified by RNA-seq and RNC-seq in HFD and HB groups. (E) Correlation between mRNA and RNC-mRNA abundance in the HFD and HB groups. Each point represents a gene sequenced by RNA-seq and RNC-seq. (F) Distribution of the RNC-mRNA abundance in HFD and HB groups. Genes were classified based on their rounded log2 RPKM abundance. Each bar represents the gene count detected by RNC-seq in each category.

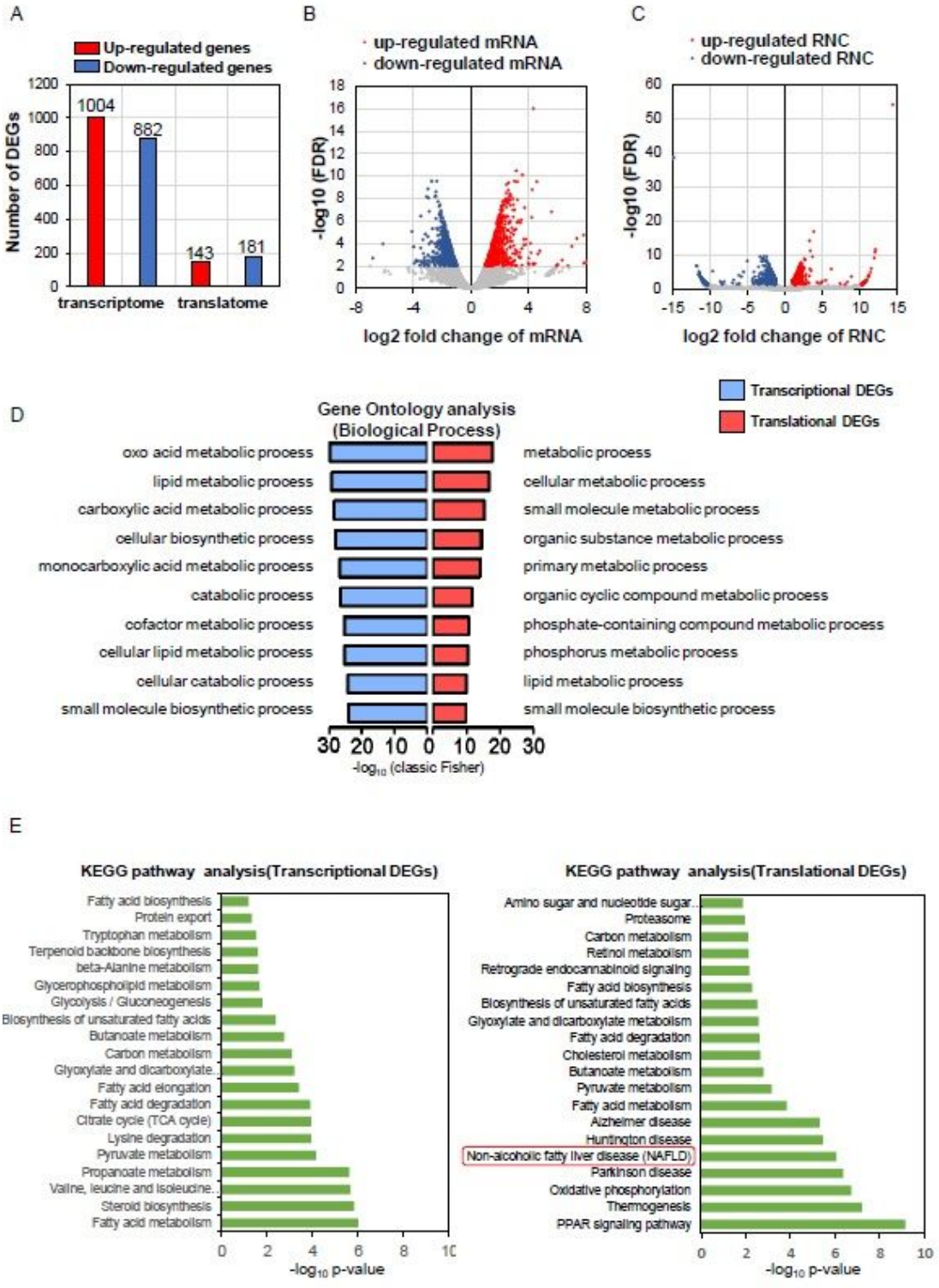

Figure 3

Analysis of differentially expressed genes at transcription level and translation level (A) Statistics of differentially up- and down-expressed gene in transcriptome and translatome. (B) Volcano map: | log2 fold change of mRNA | > 1, FDR < 0.01 as the threshold value, the differentially expressed mRNAs were screened. (C) Volcano map: | log2 fold change of mRNA | > 1, FDR < 0.05 as the threshold value, the differentially expressed RNC-mRNA were screened. (D) Pyramid figure The transcriptional and translational DEGs were analyzed by Gene Ontology (GO), and their TOP10 biological processes were ranked by -log10 (classic Fisher), The enrichment p-value of the terms ID used Fisher's exact test. (E) The transcriptional and translational DEGs were analyzed by Kyoto Encyclopedia of Genes and Genomes (KEGG), and their TOP20 pathways were ranked by -log10 (p-value).

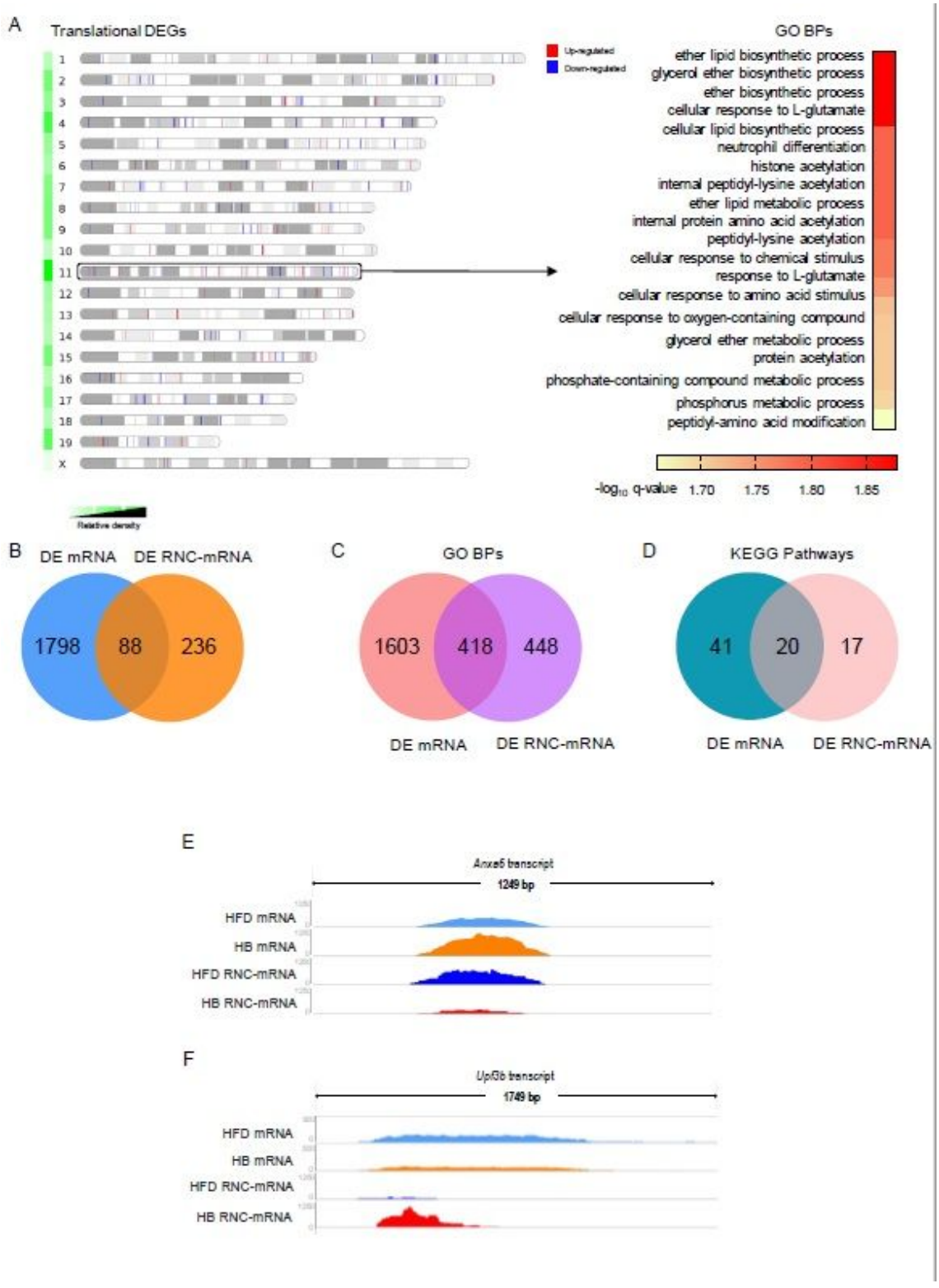

Figure 4

Further analysis of DE mRNA and DE RNC-mRNA (A) Left: Distribution of translational DEGs across chromosomes. A heat map showing relative coverage of translational DEGs in each chromosome standardized according to the length of each chromosome. Right: significantly enriched GO biological processes (BPs) by translational DEGs in chromosome 11. (B) Venn diagram of differentially expressed mRNAs (DE mRNAs) and RNC-mRNAs (DE RNC-mRNAs). (C) Venn diagrams of significantly enriched GO

BPs by DE mRNAs and DE RNC-mRNAs. (D) Venn diagrams of significantly enriched KEGG pathways by DE mRNAs and DE RNC-mRNAs. (E and F) IGV analysis at transcription level and translation level. Two examples showing the different direction of regulation between transcriptome and translatome. Two biological replicate tracks were overlaid into one. (E) Anxa6 was up-regulated at the mRNA level but down-regulated at the RNC-mRNA level. (F) While Upf3b was down-regulated at the mRNA level but up-regulated at the RNC-mRNA level.

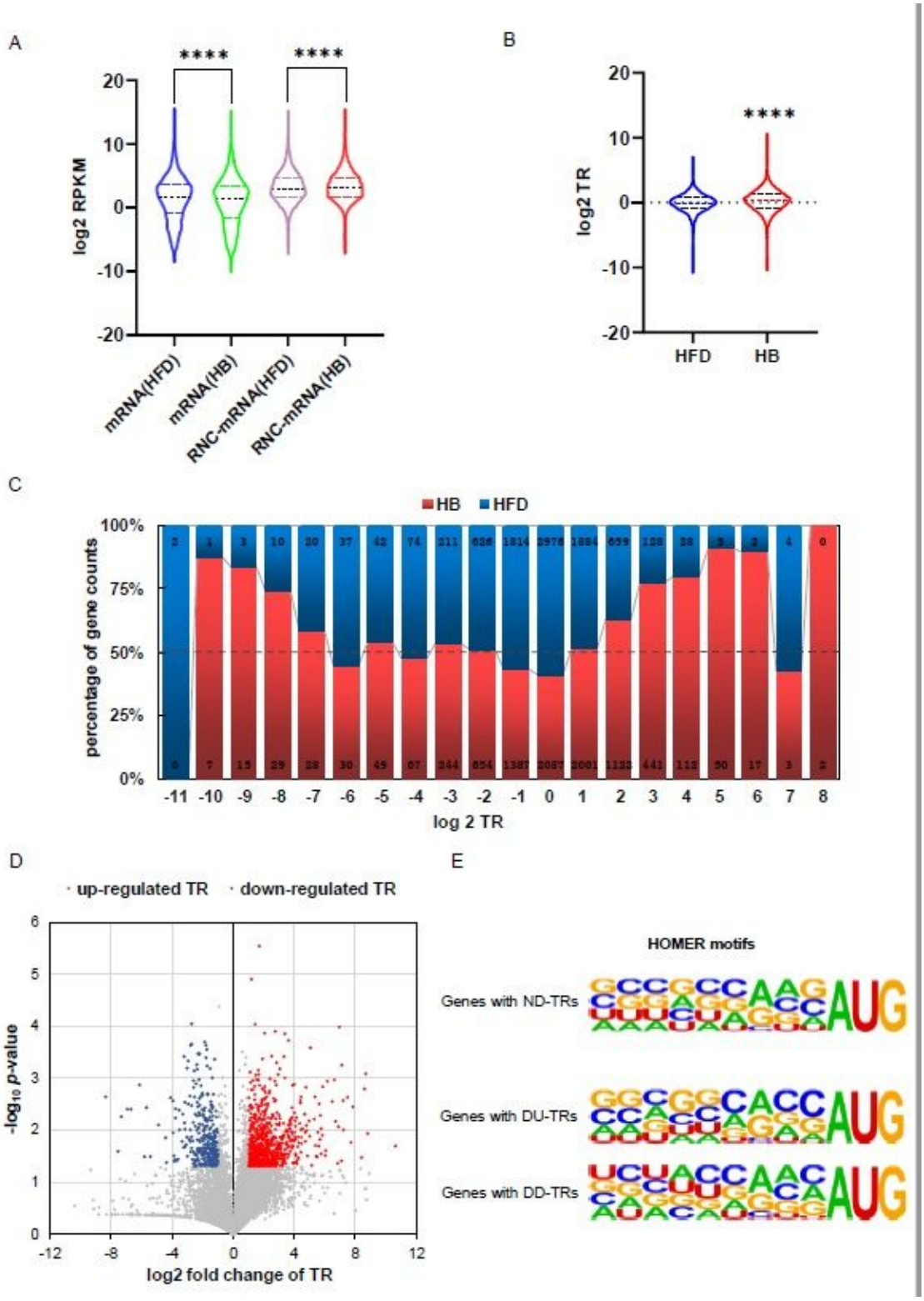

Figure 5

Translation ratio analysis (A) Violin plot of mean abundance in mRNA and RNC-mRNA of HFD group and HB group (The gene abundance is represented by log2 RPKM. ****p < 0.0001, one-way analysis of variance ANOVA). (B) Violin plot of TR in HFD and HB groups. ****p < 0.0001, student's t-test. (C) Relative TR distribution. Genes were classified based on their rounded log2 TR values. For HFD or HB groups in each category, every bar represents the percentage of the gene counts in this group to the total gene count. (D) Volcano map: | log2 fold change of mRNA | > 1, p-value < 0.01 as the threshold value, the differentially regulated TRs were screened. (E) Sequence composition between TR-differentially-up and -down-regulated genes around the AUG start codon.

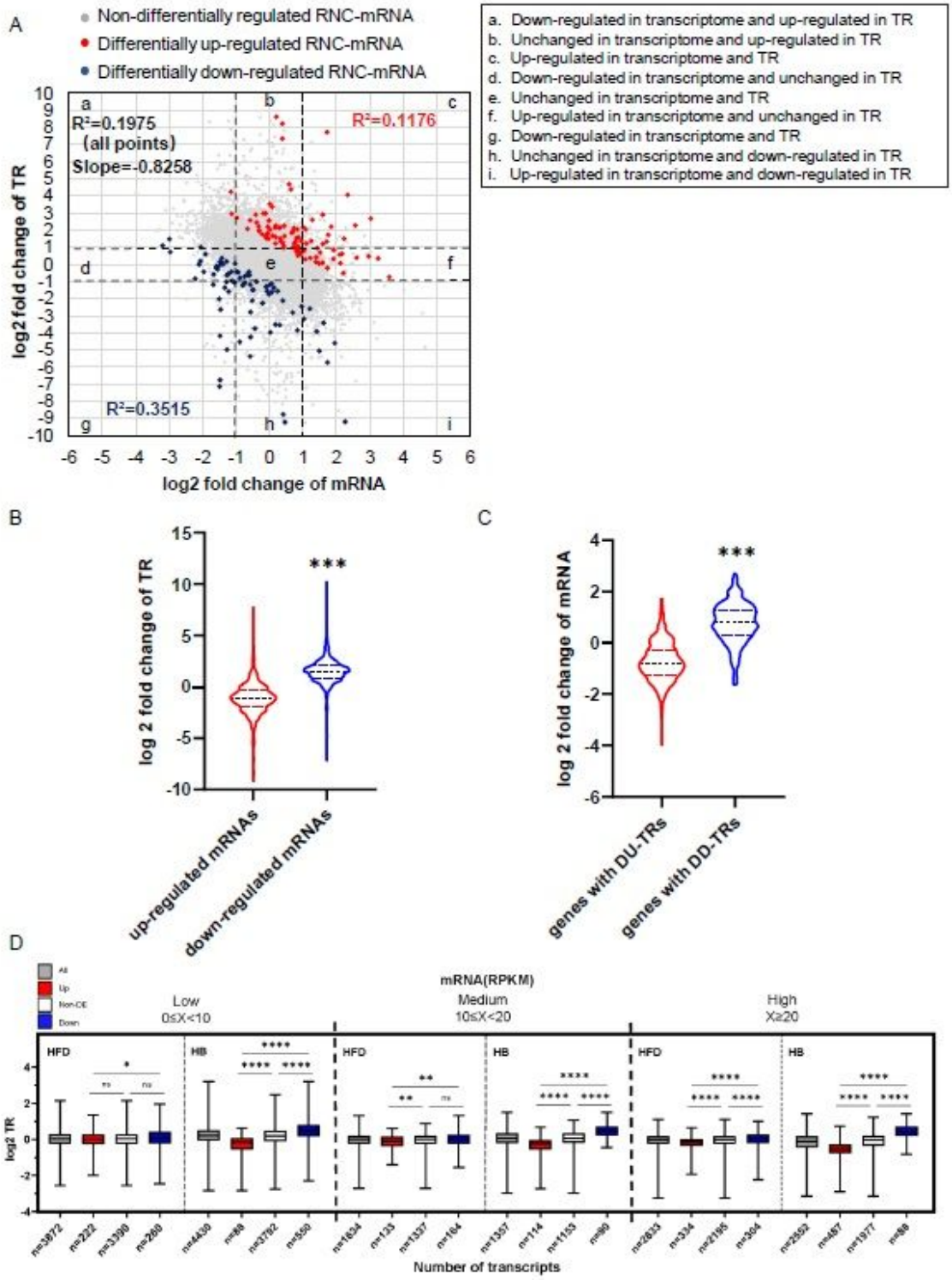

Figure 6

Correlation between transcriptional and translational regulation, in the HB group versus HFD group (A) Correlation of the fold change of mRNA abundance and TRs. Nine squares indicate nine corresponding categories. (B) Relative fold change of TR distribution of differentially regulated mRNAs. ***p < 0.001, student's t-test. (C) mRNA fold change value distribution in genes with differentially regulated TRs. ***p <

0.001, student's t-test. (D) Distribution of TR values corresponding to transcripts with different expression levels. *p < 0.05, **p < 0.01, ****p < 0.0001, one-way analysis of variance ANOVA.

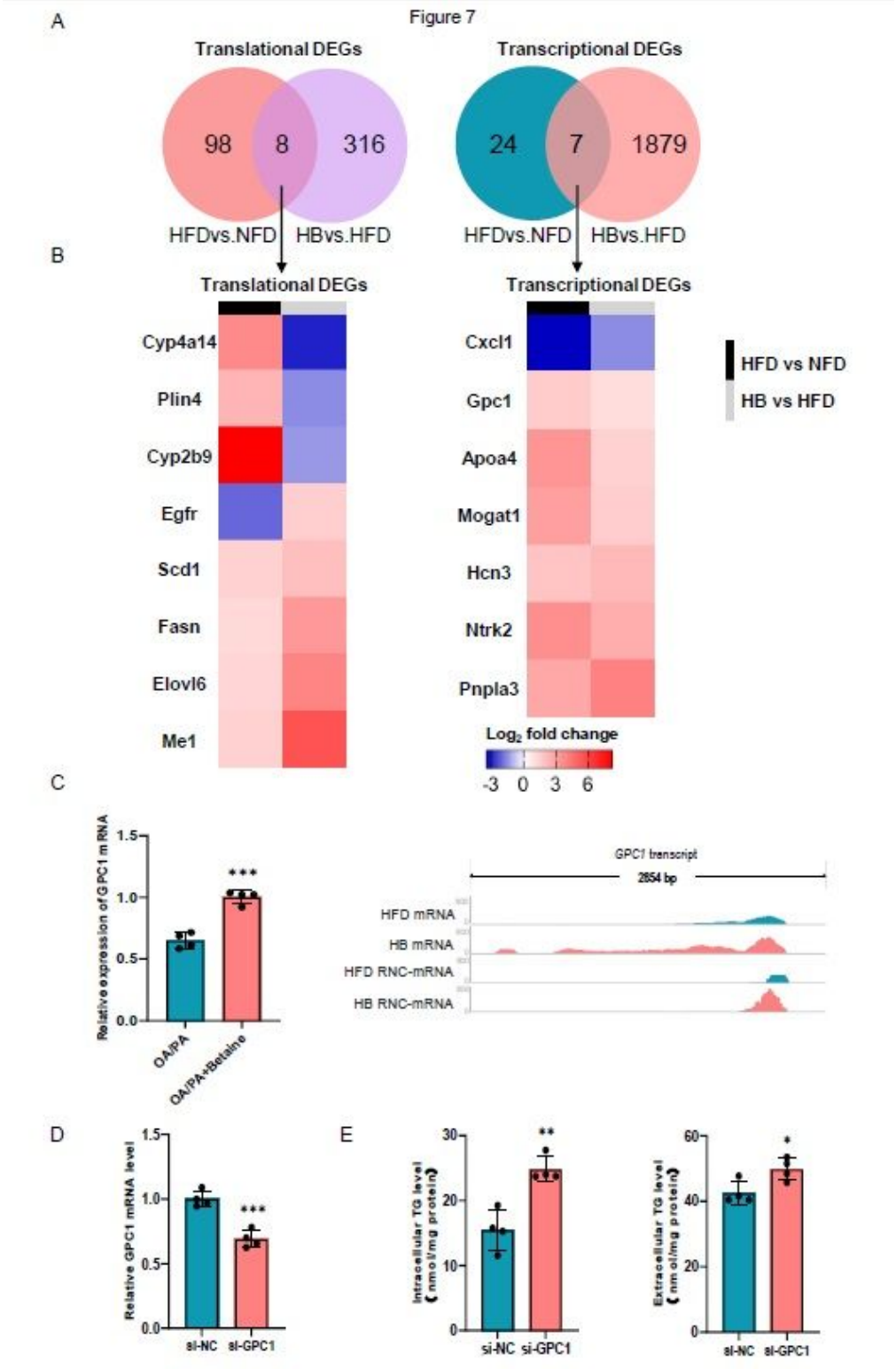

Figure 7

Functional gene screening and functional verification (A) Left: Venn diagrams: Intersection of translational DEGs in HFD vs. NFD and translational DEGs in HB vs. HFD. Right: Venn diagrams: Intersection of transcriptional DEGs in HFD vs. NFD and transcriptional DEGs in HB vs. HFD. (B) List of

screened candidate genes. In comparisons of HFD vs. NFD and HB vs. HFD, genes with different regulation were selected, both at the transcriptome and translatome. (C) Left: Relative level of Gpc1 mRNA expression in HepG2 cells in the OA/PA and OA/PA + Betaine group (n = 4). Error bars represent the standard error of the mean. ***p < 0.001, the Student's t-test. Right: IGV analysis at transcription level and translation level, Gpc1 was up-regulated at the transcriptome and translatome. (D) Relative level of Gpc1 mRNA expression in HepG2 cells transfected with siRNA, compared to the controls (NC) (n = 4). Error bars represent the standard error of the mean. ***p < 0.001, the Student's t-test. (E) Intracellular and extracellular TG concentration in Gpc1 knockdown cells (n = 4). Error bars represent the standard error of the mean. *p < 0.05, **p < 0.01, the Student's t-test.

Supplementary Files

This is a list of supplementary files associated with this preprint. Click to download.

- supplementtableS1S2.7z
- FigureS1.jpg
- FigureS2.jpg